Preferred citation: T. Saksa, J. Jeronen, N. Banichuk and M. Kurki. On travelling web stability including material viscoelasticity and surrounding air. In **Advances in Pulp and Paper Research, Cambridge 2013**, *Trans. of the XVth Fund. Res. Symp. Cambridge, 2013*, (S.J. I'Anson, ed.), pp 449–468, FRC, Manchester, 2018. DOI: 10.15376/frc.2013.1.449.

ON TRAVELLING WEB STABILITY INCLUDING MATERIAL VISCOELASTICITY AND SURROUNDING AIR

Tytti Saksa[1], Juha Jeronen[1], Nikolay Banichuk[1,2] and Matti Kurki[3]

[1] Department of Mathematical Information Technology, P.O. Box 35 (Agora), FI-40014 University of Jyväskylä, Finland, tytti.saksa@jyu.fi, juha.jeronen@jyu.fi

[2] Institute for Problems in Mechanics, Russian Academy of Sciences, Prospekt Vernadskogo 101, 119526 Moscow, Russia, banichuk@ipmnet.ru

[3] JAMK University of Applied Sciences, P.O. Box 207, FI-40101 Jyväskylä, Finland matti.kurki@jamk.fi

ABSTRACT

The aim of this research is to gain more understanding of the physics of the transportation of materials having viscoelastic characteristics, high transport speeds, a small thickness and a large surface area. This study introduces new models that take into account both material viscoelasticity and the fluid-structure interaction between the travelling material and the surrounding flowing fluid. A web (continuum) travelling between two fixed supports is considered, modelling the web as a Kelvin–Voigt type viscoelastic panel and the air flow as a potential flow. Stability of the system is studied with the help of its eigenfrequencies (eigenvalues) for two different types of flow geometries. First, a flow inside an enclosure with a rectangular cross-direction, through which the panel is travelling, is added to the equations of out-of-plane motion of the panel with the help of added mass coefficients. Secondly, a free stream potential flow obstructed

by the travelling panel is analyzed using the analytical solution for the aerodynamic reaction pressure. Some numerical examples are given for both models.

INTRODUCTION

In this study, we address questions concerning the stability of axially moving materials involving high transport speeds. Examples of such processes in industry are manufacturing of paper, steel or textiles, etc.

The analysis that will be presented can be applied in any process with axially moving plate-like materials, but our viewpoint is especially paper web handling processes with wide and thin webs. This study is among the first studies on the moving web, in which both material viscoelasticity and the interaction between the web and the surrounding fluid (air) have been included in the model.

It is well known that a high transport speed of axially moving material may lead to loss of stability resulting in damage or even breakage of the material being processed. The models used for simulating the transverse motion of travelling materials include strings, membranes, beams, panels and plates. The stability of these models has often been studied by dynamic modal analysis, i.e. by studying the eigenfrequencies of the system.

Archibald and Emslie [1] and Simpson [2] studied the effects of axial motion on the frequency spectrum and eigenfunctions. Both the travelling string and beam were shown to experience divergence instability at a sufficiently high velocity. It was also observed that the natural frequency of each eigenmode decreases as the transport velocity is increased. Wickert and Mote studied the stability of axially moving strings and beams, presenting analytical expressions for the critical transport velocities [3]. They used modal analysis and a Green's function method. Recently, Wang et al. showed that no static instability occurs at the critical velocity in the case of a string model [4]. Kong and Parker found closed-form expressions for the approximate frequency spectrum via perturbation analysis in their study concerning axially moving beams with small flexural stiffness [5].

For thin and wide webs, interaction with surrounding air affects significantly the behaviour of the travelling material. Especially in the case of travelling paper webs, the effects of the air are important, see e.g. Kulachenko et al. [6, 7] and Pramila [8].

Pramila and Niemi published a series of papers during 1986 and 1987 concerning the interaction between the travelling paper web and the external medium, using at first the analytical added-mass approximation and then the

finite element method [9, 8, 10, 11]. These studies by Pramila and Niemi are considered first studies in which fluid-structure interaction has been taken into account in the context of axially moving webs. In their studies, it was found that the presence of air reduces the values of the eigenfrequencies and critical velocities drastically compared to the vacuum case. The presence of air may reduce both to about 15–26 % of the vacuum case [8]. However, the model that was used, was later interpreted by Pramila to mean that the fluid particles move with the travelling web, which probably is not the actual physical case there [10]. Recently, Frondelius et al. used an added mass model with non-constant coefficients derived via boundary layer theory [12]. However, for this approach to be applicable, one needs to include a leading edge assumption in the fluid flow model.

Chang and Moretti further developed the added mass approach for axially moving webs comparing also their theory to their wind-tunnel experiments for stationary webs surrounded by flowing air [13]. They modelled the web as an ideal membrane and the surrounding air was treated using potential flow theory. Kulachenko modelled the fluid-structure interaction on the basis of acoustic theory finding also that the presence of air reduces the eigenfrequencies of the web compared to the vacuum case [6]. Recently, Banichuk et al. studied the interaction between the moving web and flowing air using a panel model (a plate with cylindrical deformation) and an analytical expression for the aerodynamic reaction pressure [14, 15]. The aerodynamic reaction was solved analytically for potential flow in the complex plane where the panel was represented as a cut. Eigenfrequencies and dynamic behaviour of this model were further investigated by Jeronen [16].

Industrial materials usually have viscoelastic characteristics [17], and consequently, viscoelastic moving materials have been recently studied widely. In paper making, wet paper webs are highly viscous, and therefore, viscoelasticity should be taken into account in the model (e.g. [18]).

Lee and Oh [19] studied critical speeds, eigenvalues, and natural modes of axially moving viscoelastic beams performing a detailed eigenfrequency analysis, and reported that viscoelasticity did not affect the critical velocity. In a recent study by Saksa et al., eigenvalues and stability characteristics of viscoelastic axially moving panels in vacuum were studied [20]. It was found numerically that if the viscosity is high enough, all modes behave in a stable manner with damped vibrations for any value of transport velocity, and no critical velocity was detected. In their study, the material derivative was used in the viscoelastic constitutive relations. Using the material derivative instead of a partial time derivative was first suggested by Mockensturm and Guo [21], and the material derivative has been used in most of the recent studies concerning axially moving viscoelastic beams, e.g. [22, 23].

Previous studies on moving viscoelastic materials interacting with surrounding fluid seem to be rather limited to the cases of beams having a circular cross-section [24, 25, 26] and to viscoelastic pipes conveying fluid [27, 28]. Recently, Saksa et al. [29] presented a model for axially moving thin webs, in which the material viscoelasticity was taken into account by the Kelvin–Voigt model and the effects of the surrounding air were approximated using an added mass approach. As a new result, they reported that the presence of the flowing air diminished the stabilizing effect of viscosity, i.e. for certain values of the parameters characterizing viscoelasticity, at some given axial velocity the panel could be stable when surrounded by stationary air but unstable when the air was flowing.

In this study, we take both material viscosity and interaction with fluid into account in the model for thin panels moving axially at a high speed. We model the surrounding air using both the added mass approach and a free stream potential flow. These models lead to a partial differential equation and an integro-differential equation, respectively, of the fifth order in space. We use the term *panel* for a two-dimensional web with the assumption that the transverse displacement of the web does not vary in the direction perpendicular to the direction of axial motion of the web. Using the dynamic stability analysis approach due to Bolotin [30], the behaviour of the panel is analyzed with the help of its complex eigenvalues (eigenfrequencies) with respect to the axial velocity of the panel. The analysis determines both the (real-valued) eigenfrequencies and the stability across the range of axial velocities studied. For numerical solution, the problems are discretized via the finite element method using fifth-degree Hermite polynomials with C^2 continuity. We compare the results obtained from the two different models to each other and also to previous results [29] obtained using the finite difference method.

PROBLEM SETUP

In this section, we present a model for a travelling web (continuum), restricting the consideration to one open draw. The web is mechanically supported at the inflow and outflow ends of the span, with the rest of the span unsupported. We represent the dynamical equations describing the out-of-plane mechanical behaviour of the web, based on Newton's second law and a rheological model for material viscoelasticity.

Consider an axially moving panel, travelling between two fixed supports at a constant velocity V_0. Let us make the simplifying assumption that the transverse displacement does not vary in the y (width) direction. The panel is supported at $x = -l$ and $x = l$, and the length of the span is $2l$. The transverse displacement of the panel is denoted by the function $w = w(x, t)$. The width of the panel is denoted by b, and the thickness of the panel by h. See Figure 1.

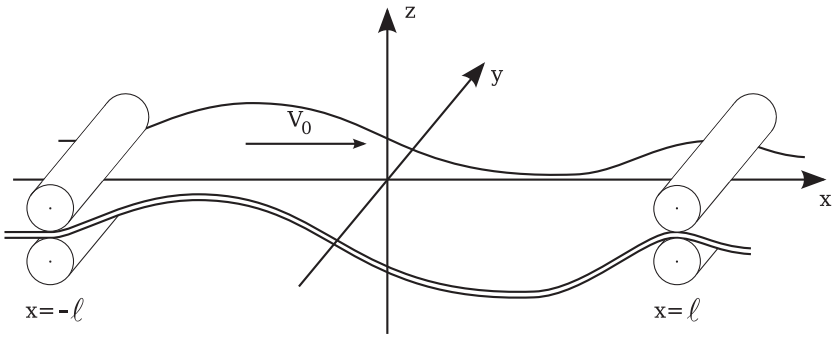

Figure 1. An axially moving panel.

The mass per unit area of the web is denoted by m. We assume constant tension at the panel ends denoted by T_0.

Viscoelasticity is taken into account by using the one-dimensional Kelvin–Voigt model (in the x direction) consisting of an elastic spring and a viscous damper connected in parallel. However, because the material is originally two-dimensional before the panel simplification is made, Poisson ratios will be included. The spring element is described by the Young's modulus, E and elastic Poisson ratio, ν, and the damper by the viscous damping coefficient, η, and the Poisson ratio for viscosity, μ. See Figure 2.

The dynamic equilibrium for the transverse displacement w in vacuum can be written as (see e.g. [20])

$$\begin{aligned} mw_{,tt} + 2V_0 mw_{,xt} + t_R Dw_{,xxxxt} \\ + (mV_0^2 - T_0)w_{,xx} + Dw_{,xxxx} + V_0 t_R Dw_{,xxxxx} = 0\,, \end{aligned} \tag{1}$$

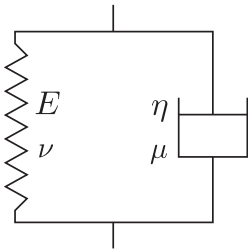

Figure 2. Kelvin–Voigt type rheological model.

where the subscripts after a comma indicate partial derivatives, e.g. $w_{,xt} \equiv \partial^2 w / \partial x \partial t$. In equation (1), D is the bending rigidity of the panel defined as

$$D = \frac{Eh^3}{12(1-\nu^2)},$$

and t_R is the retardation time constant [31] (also known as the creep time constant) defined as

$$t_R = \frac{\eta}{E},$$

the SI unit of which is the second. We have assumed that the elastic and viscous Poisson ratios ν and μ coincide.

The boundary conditions for (1) are set as

$$w(-\ell,t) = w_{,x}(-\ell,t) = w_{,xx}(-\ell,t) = 0 \quad \text{and} \quad w(\ell,t) = w_{,x}(\ell,t) = 0\,. \qquad (2)$$

Again the subscripts after a comma indicate partial derivatives. For derivation of the boundary conditions, see [20].

Equation (1) together with the boundary conditions (2) describes the out-of-plane displacement of the panel moving at a constant axial velocity V_0 through a span of length $2l$. Further below, we will study these equations with the help of dynamic analysis separating a known time-dependent part. Thus, we will not study the full time-dependent equation (1), but will instead investigate a certain type of behaviour that is important with regard to the stability of the moving panel. To solve the full equation, one would also need to set two initial conditions in addition to the boundary conditions (2).

In the following, we will consider two flow models: a panel travelling through an enclosure, and a panel subjected to an axial free-stream flow.

Panel travelling through an enclosure with a rectangular cross-section

In the first model, we let the panel travel through a long enclosure with a rectangular cross-section, to model a web travelling through a drying oven. The height of the enclosure is H and its width is B. The velocity field of the fluid is denoted by U. See Figure 3. Note that the rollers in the figure only express the web being supported along the lines $x = -l$ and $x = l$. In the flow model, the rollers are not accounted for.

Following Chang and Moretti [13], we include added masses due to the transverse, Coriolis and centripetal acceleration (i.e. in all inertia terms) denoted by m_1, m_2, and m_3, respectively.

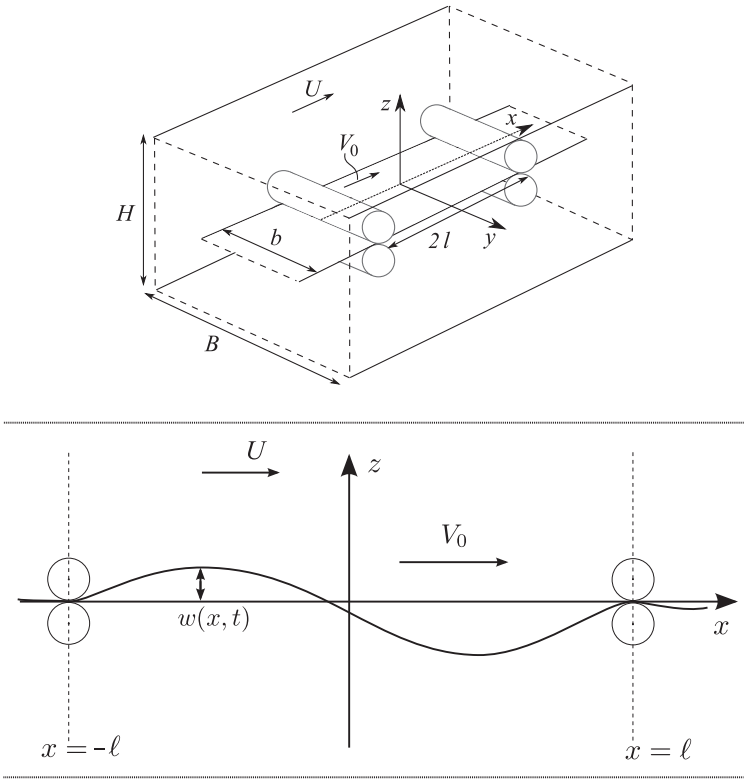

Figure 3. An axially moving panel submerged in flowing fluid.

Inserting the added masses into (1), we obtain the dynamic equation for the travelling panel interacting with the surrounding air:

$$\begin{aligned}(m+m_1)w_{,tt} + 2V_0(m+m_2)w_{,xt} + t_{\mathrm{R}}Dw_{,xxxxt} \\ + [(m+m_3)V_0^2 - T_0]w_{,xx} + Dw_{,xxxx} + V_0 t_{\mathrm{R}}Dw_{,xxxxx} = 0\,.\end{aligned} \tag{3}$$

The added mass terms in (3) can be calculated as [13]

$$m_1 = \frac{\pi}{4}\mathrm{C_a}\rho_{\mathrm{f}}b\,, \qquad m_2 = 2\rho_{\mathrm{f}}\delta^*\,, \qquad m_3 = 2\rho_{\mathrm{f}}\theta\,,$$

where C_{a} is the added mass coefficient depending on the problem geometry, ρ_{f} is the density of the surrounding air, δ* is the displacement thickness of the boundary layer and θ is the momentum thickness of the boundary layer.

If $U = U(r)$ is the velocity of the fluid flow with respect to the distance r from the panel, δ^* and θ are given by

$$\delta^* = \frac{1}{V_0}\int_0^{\delta} U(r)\,\mathrm{d}r\,, \qquad \theta = \frac{1}{V_0^2}\int_0^{\delta} U^2(r)\,\mathrm{d}r\,,$$

where δ is the thickness of the moving fluid layer [13].

If the fluid velocity profile $U(r)$ is known, δ^* and θ can be determined, and values obtained for the added masses m_i for $i = 1, 2, 3$. Equation (3) with the boundary conditions (2) (given above) describes the behaviour of the panel travelling through an enclosure.

Travelling panel submerged in a free stream flow

Now let us consider the second model. Let the panel travel in an unlimited space with axial flow surrounding it. Since the panel model is onedimensional, the surrounding flow is two-dimensional, and the domain of the fluid flow is the infinite xz plane with the part representing the panel removed.

The axial flow is modelled as a free stream potential flow. The free stream velocity is denoted by v_∞. See Figure 4. Again, the rollers in the figure only express the web being supported at $x = -l$ and $x = l$, and are not part of the flow model.

The free stream velocity is allowed to be either zero (to model stationary air) or nonzero. It is also possible to set $v_\infty = V_0$, in which case the surrounding free stream follows the axial motion of the moving panel.

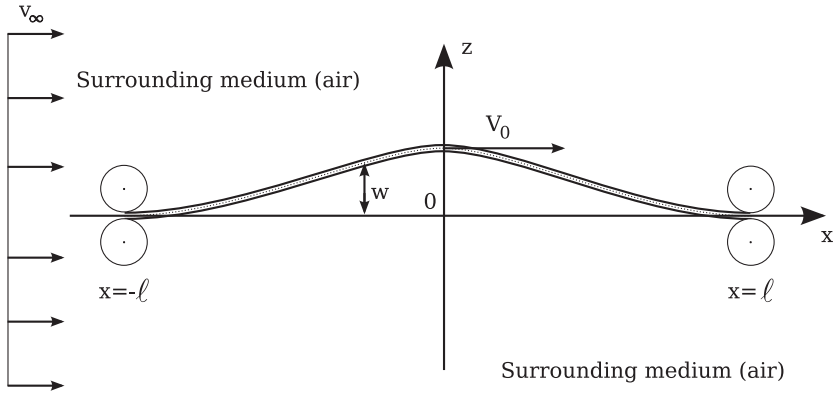

Figure 4. A travelling panel submerged in a free stream potential flow.

The equation for the out-of-plane motion of the travelling panel is now written with the help of the aerodynamic reaction pressure q_f:

$$\begin{aligned} mw_{,tt} + 2V_0 mw_{,xt} + t_R D w_{,xxxxt} \\ + (mV_0^2 - T_0) w_{,xx} + D w_{,xxxx} + V_0 t_R D w_{,xxxxx} + q_f = 0 \,. \end{aligned} \tag{4}$$

We assume nonstationary aerodynamic flow in the xz plane (Figure 4). The reaction pressure q_f exerted by the fluid can be expressed as

$$q_f(x,t) = \rho_f \left(\frac{\partial}{\partial t} + v_\infty \frac{\partial}{\partial x} \right) \left(\varphi^+(x,t) - \varphi^-(x,t) \right) \,, \tag{5}$$

where φ^- and φ^+ denote the limits

$$\varphi^\pm(x,t) = \lim_{z \to 0^\pm} \varphi(x,z,t) \,,$$

and φ is the aerodynamic disturbance velocity potential, describing the non-freestream component of fluid motion, due to the solid obstacle. As before, in (5) the constant ρ_f denotes the density of the surrounding air.

The aerodynamic disturbance potential φ can be determined analytically by solving the Laplace equation for φ in the xz plane from which the part $z = 0$, $-1 \le x \le 1$ is cut. If we assume that the panel displacement w and its derivatives are small, in the flow geometry it is possible to approximate the panel as being perfectly flat (whence $z = 0$ in the cut), and account for the shape and the motion of the panel only through the boundary condition which states that no flow occurs through the panel surface. This is sufficient for the analysis of small vibrations and stability. See [15] for details.

To present the solution, we first introduce the dimensionless coordinates x', t' and the dimensionless displacement function w':

$$x' = \frac{x}{\ell} \,, \qquad t' = \frac{t}{\tau} \,, \qquad w'(x',t') = \frac{w(x,t)}{\ell} \,. \tag{6}$$

Here l is half the span length. The constant τ is called the characteristic time and it can be chosen freely.

The aerodynamic problem for the potential flow surrounding the panel is now written as

$$\begin{aligned} &\Delta\varphi = 0 \,, \\ &\left(\frac{\partial \varphi}{\partial z} \right)^\pm = \frac{\ell}{\tau} \frac{\partial w'}{\partial t'} + v_\infty \frac{\partial w'}{\partial x'} \qquad -1 \le x' \le 1, \quad z = 0 \,, \\ &\lim_{|(x,z)| \to \infty} \nabla\varphi = 0 \,. \end{aligned} \tag{7}$$

Solving the aerodynamic problem (7) (see [15] for details) and inserting the solution into (5), we obtain the analytical expression for $q_f(x, t)$:

$$q_f(x,t) = -\rho_f \left(\frac{\ell}{\tau}\frac{\partial}{\partial t'} + v_\infty \frac{\partial}{\partial x'} \right) \int_{-1}^{1} N(\xi, x') \left(\frac{\ell}{\tau}\frac{\partial}{\partial t'} + v_\infty \frac{\partial}{\partial \xi} \right) w'(\xi, t') \mathrm{d}\xi \,, \quad (8)$$

where the kernel function N is

$$N(\xi, x') = \frac{1}{\pi} \ln \left| \frac{1 + \Lambda(\xi, x')}{1 - \Lambda(\xi, x')} \right| , \quad (9)$$

$$\Lambda(\xi, x') = \left[\frac{(1 - x')(1 + \xi)}{(1 - \xi)(1 + x')} \right] . \quad (10)$$

In (8), ξ is a dummy variable of integration. We have used the dimensionless displacement w'. Comparing (8) with the expression in [15], in which the dimensional displacement w was used, there is an additional multiplication by $1/l$. Noting that $w = lw'$, the expressions agree.

We have thus obtained the aerodynamic pressure q_f, which describes the pressure difference generated over the panel surface, as the surrounding flow reacts to the shape and the motion of the panel. Since the response can be presented analytically with the help of the displacement function w, we have only one equation (after inserting (8) into (4)) that describes the behaviour of the panel. As before, the boundary conditions are (2), given further above.

DIMENSIONLESS FORMS

We now have two problems, one for each flow model considered. The problem (2), (3) describes the behaviour of the panel travelling through an enclosure, while the problem (2), (4) describes the behaviour of the panel travelling in a surrounding axial free stream flow.

For the purpose of numerical analysis, we present the problems (2), (3) and (2), (4) in a dimensionless form, which is a standard preparation step when numerically working with partial differential equations describing physical phenomena. The dimensionless form minimizes the number of independent parameters in the mathematical problem, and in some cases also facilitates the use of a reference domain for computations. For example, in the second model, by using dimensionless variables, the solution (8) can be directly applied without modification for any physical span half-length l.

Let us choose the characteristic time τ in (6) as follows:

$$\tau = \ell\sqrt{\frac{m}{T_0}}\,. \tag{11}$$

We now introduce the following dimensionless problem parameters:

$$c = \frac{V_0}{\sqrt{T_0/m}}\,, \qquad \theta = \frac{v_\infty}{\sqrt{T_0/m}}\,, \tag{12}$$

$$\alpha = \frac{D}{\ell^2 T_0}\,, \qquad \beta = \frac{\ell\rho_{\mathrm{f}}}{m}\,, \qquad \gamma = \frac{t_{\mathrm{R}}}{\tau} = \frac{\eta}{E}\frac{\sqrt{T_0}}{\ell\sqrt{m}}\,, \tag{13}$$

$$\zeta = \frac{m}{m+m_1}\,, \qquad \zeta_2 = \frac{m+m_2}{m+m_1}\,, \qquad \zeta_3 = \frac{m+m_3}{m+m_1}\,, \tag{14}$$

Above, γ is called the dimensionless retardation time.

We will first rewrite the dynamic equation in the case of the added mass approach, i.e. problem (2), (3). Inserting (6) into (3), using the dimensionless parameters in (12)–(14) and omitting the primes from the dimensionless coordinates, we obtain

$$\begin{aligned} w_{,tt} + 2c\,\zeta_2 w_{,xt} + \gamma\alpha\zeta w_{,xxxxt} \\ + (c^2\zeta_3 - \zeta)w_{,xx} + \alpha\zeta w_{,xxxx} + \gamma\alpha c\zeta w_{,xxxxx} = 0\,. \end{aligned} \tag{15}$$

Note that equation (15) also describes the vacuum case, by setting $\zeta = \zeta_2 = \zeta_3 = 1$ (i.e. no added mass, $m_1 = m_2 = m_3 = 0$).

For the dynamic equation of the travelling panel submerged in a free stream potential flow, i.e. problem (2), (4), we proceed in a similar manner.

We insert (6) into (4), use the dimensionless parameters in (12)–(13) and finally omit the primes from the dimensionless variables, obtaining

$$\begin{aligned} w_{,tt} + 2cw_{,xt} + \gamma\alpha w_{,xxxxt} \\ + (c^2-1)w_{,xx} + \alpha w_{,xxxx} + \gamma\alpha c w_{,xxxxx} \\ + \beta\left(\frac{\partial}{\partial t} + \theta\frac{\partial}{\partial x}\right)\int_{-1}^{1} N(\xi,x)\left(\frac{\partial}{\partial t} + \theta\frac{\partial}{\partial \xi}\right) w(\xi,t)\mathrm{d}\xi = 0\,. \end{aligned} \tag{16}$$

Setting $\beta = 0$ in (16) gives us the vacuum case.

We make the insertion of (6) also to the boundary conditions (2) and get

$$w(-1,t) = w_{,x}(-1,t) = w_{,xx}(-1,t) = 0 \quad \text{and} \quad w(1,t) = w_{,x}(1,t) = 0\,. \tag{17}$$

We now have the dimensionless forms for the panel behaviour using both flow models. The problem (15), (17) describes the behaviour of the panel travelling through an enclosure, while the problem (16), (17) corresponds to the panel travelling in a surrounding axial free stream flow.

DYNAMIC ANALYSIS

In this section, we briefly describe the method that is often (and also here) used in the analysis of time-dependent partial differential equations. We will analyze the boundary value problems (15), (17) and (16), (17) via their eigenvalues. With the help of the eigenvalues, it is possible to study the characteristic behaviour for different values of problem parameters, and to make systematic parametric studies.

In the present study, the goal of this analysis is to investigate the dynamical stability of the system, and to find the lowest critical velocity for axial web motion, up to which the system behaves in a stable manner. The result is a theoretical stability limit for stable web motion in real open draws, such as are encountered in actual paper machines.

Furthermore, the analysis produces the characteristic frequencies of free vibrations of the paper web in a given open draw, i.e. those frequencies at which the system may resonate, at least according to the model where small vibrations are assumed.

To study the dynamical stability of the problems (15), (17) and (16), (17), we perform classical dynamic stability analysis [30] by inserting the standard time-harmonic trial function

$$w(x,t) = W(x)e^{st}\,, \tag{18}$$

into the dimensionless form of the problem. In (18),

$$s = i\omega\,,$$

where ω is the dimensionless angular frequency of small transverse vibrations.

The (complex-valued) quantity s is called the stability exponent. The sign of the real part of s characterizes the stability of the system. If $\mathrm{Re}\, s > 0$, the behaviour is unstable, and otherwise it is stable. This classification is based on two important properties. For any linear differential equation, the real and imaginary parts of the solution (18) are also solutions of the same equation. Hence the complex-valued solution immediately gives physically admissible real-valued solutions. The other property is that if $\mathrm{Re}\, s > 0$, via the use of Euler 's formula (in complex analysis)

one can split the complex-valued exp into the product of a harmonic vibration (or as a special case, a constant) with a real-valued exponential that grows with increasing t. Thus, if the system finds itself in a state where Re $s > 0$, the model predicts that the vibrations will grow without bound, leading to dynamical instability.

Inserting (18) into the dimensionless added mass problem (15), (17) we obtain

$$s^2 W + s(2c\,\zeta_2 W_{,x} + \gamma\alpha\zeta W_{,xxxx}) + (c^2\zeta_3 - \zeta)W_{,xx} + \alpha\zeta W_{,xxxx} + \gamma\alpha c\zeta W_{,xxxxx} = 0\,. \qquad (19)$$

We proceed similarly in the case of free stream potential flow. Insertion of (18) into (16) gives

$$s^2 W + s(2cW_{,x} + \gamma\alpha W_{,xxxx}) + (c^2 - 1)W_{,xx} + \alpha W_{,xxxx} + \gamma\alpha c W_{,xxxxx} + \beta\left(s + \theta\frac{\partial}{\partial x}\right)\int_{-1}^{1} N(\xi, x)\left(s + \theta\frac{\partial}{\partial \xi}\right) W(\xi, t)\mathrm{d}\xi = 0\,. \qquad (20)$$

The boundary conditions for W in (19) and (20) are

$$W(-1) = W_{,x}(-1) = W_{,xx}(-1) = 0\,, \qquad W(1) = W_{,x}(1) = 0\,. \qquad (21)$$

We have reduced both problems into a form with no explicit time dependence; what remains is a boundary value problem for an ordinary differential equation in x. The problem (15), (17) has been reduced into the problem (19), (21), and the problem (16), (17) into the problem (20), (21), respectively.

The time dependence of each solution is determined by the value of s, via the $\exp(st)$ in (18). The task in the eigenvalue analysis is to simultaneously determine the unknown eigenvalue s and the corresponding solution W.

NUMERICAL EXAMPLES

We will consider two examples, one for each flow model. First, we consider a simple flow through an enclosure with a rectangular cross-section, and second the free stream potential flow. For some more results on the first model, see [29].

The problems (19), (21) and (20), (21) were discretized via the finite element method using a Hermite basis with C^2 continuity, consisting of fifth-degree polynomials. The degrees of freedom were the function value, the first derivative, and the second derivative at the nodes. A uniform grid was used with 20 elements. It

was observed that doubling the number of elements from this did not affect the values of the first three pairs of eigenvalues significantly. Note that the integral terms in the second model produce full matrices.

In the case of both considered problems, discretization leads to a quadratic eigenvalue problem with respect to s, which can be solved using standard techniques (see e.g. [32]). In the figures, the lowest three eigenvalue pairs are shown.

In the following numerical examples, the dimensionless frequency F has been calculated with the help of the dimensionless angular frequency $\omega = \mathrm{Im}\, s$.

The original, dimensional frequency f is

$$f = \frac{\omega}{2\pi\tau}. \tag{22}$$

We define the dimensionless frequency so that we divide f by the natural frequency of non-moving ideal string in vacuum, that is, by

$$f_{\mathrm{str}} = \frac{\pi/2}{2\pi\tau} = \frac{1}{4\tau}.$$

We obtain

$$F = \frac{f}{f_{\mathrm{str}}} = \frac{2\omega}{\pi} = 2\frac{\mathrm{Im}\, s}{\pi}. \tag{23}$$

The behaviour of the dimensionless frequency F is studied with respect to the dimensionless panel velocity c. Motivated by (23), in the figures both the real and imaginary parts of s have been scaled by $2/\pi$.

The material parameters used for both examples were

$$\begin{gathered} T_0 = 500\ \mathrm{N/m}, \quad m = 0.08\ \mathrm{kg/m^2}, \quad E = 10^9\ \mathrm{N/m^2}, \\ \nu = 0.3, \quad \rho_{\mathrm{f}} = 1.225\ \mathrm{kg/m^3} \end{gathered} \tag{24}$$

Let us begin with the example of the panel travelling through the drying oven. We assume a Couette type flow such that the fluid velocity coincides with the panel velocity on the panel surface and is equal to zero at the surface of the enclosure. The velocity profile is linear. See Figure 5.

Chang and Moretti [13] computed the added mass coefficient C_{a} for different simple problem geometries assuming potential flow in the cross-direction plane, obtaining the stream-function by a finite difference method. In such conditions that $H/B = 0.4$ and $b/B = 0.8$, they found that $C_{\mathrm{a}} = 1.66$.

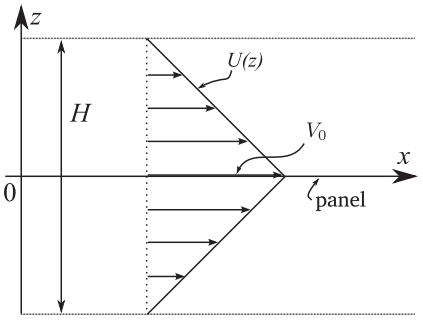

Figure 5. Couette type flow surrounding the moving web, following Chang and Moretti [13].

The used parameters related to the flow geometry were

$$\ell = 0.5\ \mathrm{m}, \quad b = 0.6\ \mathrm{m}, \quad h = 10^{-4}\ \mathrm{m},$$
$$H = 0.3\ \mathrm{m}, \quad B = 0.75\ \mathrm{m} \tag{25}$$

Two representative examples are given. The retardation time t_R is given the values $t_R = 5 \cdot 10^{-5}$ s and $5 \cdot 10^{-3}$ s. See Figure 6 for the results. In the figure, the three lowest complex eigenvalue pairs are plotted for a range of velocities around the first critical point. The real part of s characterizes the stability behaviour of the moving panel, while the imaginary part gives the

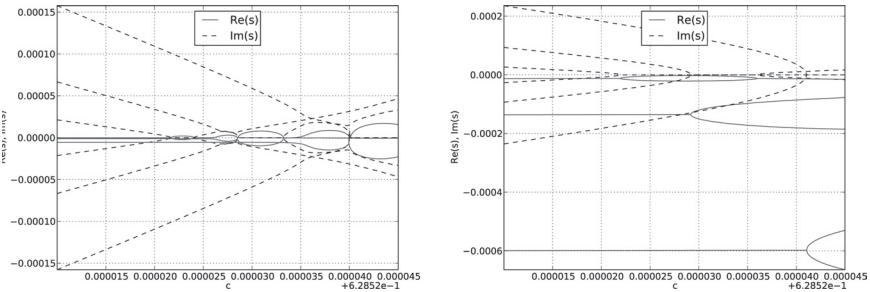

Figure 6. Behaviour of the lowest three pairs of eigenvalues for the added mass model near the first critical point. Notice the shift on the horizontal axis. *Left*: $t_R = 10^{-5}$ s. *Right*: $t_R = 10^{-3}$ s.

real-valued eigenfrequency. Negative real parts indicate damping, positive real parts instability.

The first critical point is the point where the imaginary parts of the lowest eigenvalue pair merge. In both subfigures, this occurs between the axis marks $c = 0.000020$ and $c = 0.000025$ (but note the shift on the horizontal axis).

It is observed that for the larger value of the retardation time constant t_R, the values of the eigenfrequencies increase, i.e. the natural vibration of the moving panel becomes faster than in the other case. That is, when the eigenfrequencies are considered, the material viscosity has the opposite effect to that of introducing the surrounding fluid.

Also, if the material viscosity is high enough, we see that the first critical point may become stable. In the case with $t_R = 10^{-3}$ s, the real parts of all three eigenvalue pairs remain negative. Physically, this means that a sufficiently viscous material can be driven without losing stability at velocities higher than the first critical point.

The qualitative behaviour captured here is the same as for the finite difference solution reported in [29].

Next, consider the moving panel submerged in free stream potential flow. We consider two different cases, giving two representative examples of each. The first case is with stationary fluid (no free stream, $v_\infty = 0$; in equation (20), $\theta = 0$), and in the second case, the free stream is assumed to move at the same velocity as the panel ($v_\infty = v_0$; in equation (20), $\theta = c$).

The panel dimensions used were $l = 0.5$ m and $h = 10^{-4}$ m, the same as in the added mass example. For the stationary fluid, the retardation time t_R was given the values $t_R = 5 \cdot 10^{-5}$ s and $5 \cdot 10^{-3}$ s.

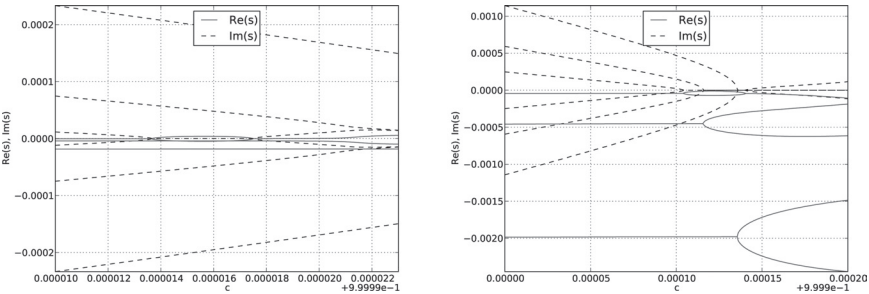

Figure 7. Behaviour of the lowest three pairs of eigenvalues for the free stream potential flow mass model near the first critical point. Stationary fluid, $\theta = 0$. Notice the shift on the horizontal axis. *Left*: $t_R = 10^{-5}$ s. *Right*: $t_R = 10^{-3}$ s.

The first critical point is found near $c = 1$. It is a property of this fluid model (see [15, 16]) that when $\theta = 0$, it does not change the critical velocity from the vacuum case, but only the eigenfrequencies are changed. Hence, the small shift in the critical point, compared to the ideal string for which the critical point occurs at $c = 1$, comes only from the bending rigidity and material viscosity contributions.

The results are qualitatively similar to those from the added mass model. For small material viscosities, the first critical point is unstable, but if the material viscosity is high enough, it becomes stable.

The same values for the retardation time were also tested for the case of the fluid moving with the panel, but the two values produced almost identical results, and hence only one is shown. Numerical tests using constant values for θ indicated that the destabilizing effect of the free-stream fluid motion (see [15]) cancels the stabilizing effect of the material viscosity. This is the case also when $\theta = c$. It seems the fluid terms dominate, rendering the results near identical. However, by further increasing the value of t_R by another factor of 100, a minor stabilizing effect reappears, but it is not strong enough to stabilize the critical point. In Figure 8, cases $t_R = 5 \cdot 10^{-3}$ s and $5 \cdot 10^{-1}$ s (the latter displaying some stabilization) are shown.

For the two cases of the moving panel submerged in free stream potential flow, the location of the first critical point matches Pramila's interpretation [10] that was mentioned at the beginning. If the free stream moves at the same velocity as the panel, the critical velocity is drastically reduced (Figure 8; note that the critical point is located between $c = 0.50$ and $c = 0.52$, and compare to the earlier examples above). Indeed, if there is no free stream, then according to this model, the critical velocity remains the same as in the vacuum case.

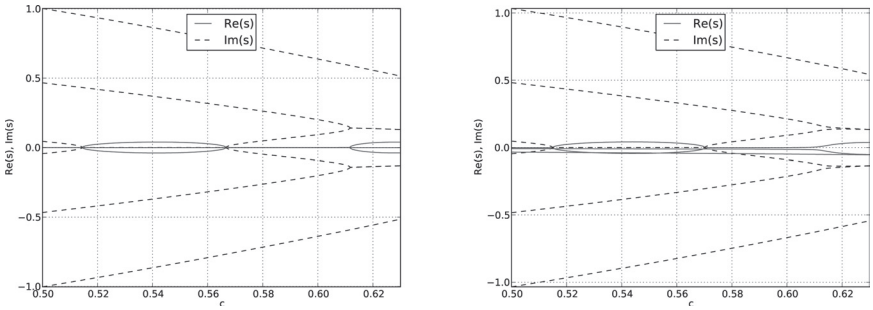

Figure 8. Behaviour of the lowest three pairs of eigenvalues for the free stream potential flow mass model near the first critical point. Fluid moves with the panel, $\theta = c$. *Left*: $t_R = 10^{-3}$ s. *Right*: $t_R = 10^{-1}$ s. Note the small asymmetry in the real parts at the right.

CONCLUSIONS

The results in this paper shed light on the behaviour of the panel model, when linear viscoelasticity and certain simple kinds of fluid flows are taken into account. From the viewpoint of mathematical modelling, the behaviour of the model near the first critical point is an interesting question with important stability implications (in the Bolotin sense).

It was seen that in most of the studied cases, the critical point is unstable, as is expected for a travelling material. As an exception, in the case of the added-mass model with high enough material viscosity, the critical point becomes stable. This result is obtainable also in the vacuum case, because the added-mass model only modifies the coefficients of the equation describing the material behaviour in vacuum. As for the potential flow model using the analytical solution of the flow problem, it was seen that when the fluid moves with the panel, then at least in the range of values that were tested for the retardation time constant t_R , there is no such stabilization effect.

The presented model has an application in modelling the behaviour of fast moving wide webs in industry, e.g. in paper making. By using measured parameter values in the model, and measuring the natural frequencies of the actual physical system at different axial velocities, it is possible to find the model where the predicted eigenfrequencies best match the measured data. Then, by examining the prediction for critical velocity from that model, it is possible to predict the critical velocity for an actual open draw. Of course, when predicting the stability limit for the whole paper machine, the smallest of all predicted critical velocities (for the different open draws) is the relevant quantity.

However, it should be noted that the models used in the present study are rather simple. For improving on the predictions made in this paper, one should notice that viscoelasticity in paper does not behave linearly and that, to take into account the complicated airflows inside the paper machine, the potential flow model is probably not accurate enough.

Especially air flows with real viscous fluid properties around the moving web seem to be very complex. Potential flow theory does not take into account the effects of fluid viscosity, and therefore the inertial time-dependent effects of non-steady-state moving webs are not accurate.

Even though in the added-mass model, the boundary layer effects were taken into account in parameters m_2 and m_3 concerning the Coriolis and centripetal terms, real time dependence and turbulent air flow around the moving, vibrating web cannot be understood using this approach. One of the possible future directions could be to investigate the dynamics of the moving web coupled with the Navier-Stokes equations.

ACKNOWLEDGMENTS

This research was supported by the Academy of Finland (grant no. 140221) and the Jenny and Antti Wihuri Foundation.

REFERENCES

1. F. R. Archibald and A. G. Emslie. The vibration of a string having a uniform motion along its length. *ASME Journal of Applied Mechanics*, 25:347–348, 1958.
2. A. Simpson. Transverse modes and frequencies of beams translating between fixed end supports. *Journal of Mechanical Engineering Science*, 15:159–164, 1973.
3. J. A. Wickert and C. D. Mote. Classical vibration analysis of axially moving continua. *ASME Journal of Applied Mechanics*, 57:738–744, 1990.
4. Y. Wang, L. Huang, and X. Liu. Eigenvalue and stability analysis for transverse vibrations of axially moving strings based on Hamiltonian dynamics. *Acta Mechanica Sinica*, 21:485–494, 2005.
5. L. Kong and R. G. Parker. Approximate eigensolutions of axially moving beams with small flexural stiffness. *Journal of Sound and Vibration*, 276:459–469, 2004.
6. A. Kulachenko, P. Gradin, and H. Koivurova. Modelling the dynamical behaviour of a paper web. Part I. *Computers & Structures*, 85:131–147, 2007.
7. A. Kulachenko, P. Gradin, and H. Koivurova. Modelling the dynamical behaviour of a paper web. Part II. *Computers & Structures*, 85:148–157, 2007.
8. A. Pramila. Sheet flutter and the interaction between sheet and air. *TAPPI Journal*, 69(7):70–74, 1986.
9. J. Niemi and A. Pramila. Vibration analysis of an axially moving membrane immersed into ideal fluid by FEM. Technical report, Tampereen teknillinen korkeakoulu (Tampere University of Technology), Tampere, 1986.
10. A. Pramila. Natural frequencies of a submerged axially moving band. *Journal of Sound and Vibration*, 113(1):198–203, 1987.
11. A. Pramila and J. Niemi. FEM-analysis of transverse vibrations of an axially moving membrane immersed in ideal fluid. *International Journal for Numerical Methods in Engineering*, 24(12):2301–2313, 1987. 1–09702–07.
12. T. Frondelius, H. Koivurova, and A. Pramila. Interaction of an axially moving band and surrounding fluid by boundary layer theory. *Journal of Fluids and Structures*, 22(8):1047–1056, 2006.
13. Y. B. Chang and P. M. Moretti. Interaction of fluttering webs with surrounding air. *TAPPI Journal*, 74(3):231–236, 1991.
14. N. Banichuk, J. Jeronen, P. Neittaanmäki, and T. Tuovinen. Static instability analysis for travelling membranes and plates interacting with axially moving ideal fluid. *Journal of Fluids and Structures*, 26(2):274–291, 2010.
15. N. Banichuk, J. Jeronen, P. Neittaanmäki, and T. Tuovinen. Dynamic behaviour of an axially moving plate undergoing small cylindrical deformation submerged in axially flowing ideal fluid. *Journal of Fluids and Structures*, 27(7):986–1005, 2011.

16. J. Jeronen. *On the mechanical stability and out-of-plane dynamics of a travelling panel submerged in axially flowing ideal fluid: a study into paper production in mathematical terms*. PhD thesis, Department of Mathematical Information Technology, University of Jyväskylä, 2011. Jyväskylä studies in computing 148. ISBN 978–951–39–4595–4 (book), ISBN 978–951–39–4596–1 (PDF).
17. R.-F. Fung, J.-S. Huang, and Y.-C. Chen. The transient amplitude of the viscoelastic travelling string: An integral constitutive law. *Journal of Sound and Vibration*, 201(2):153–167, 1997. DOI: 10.1006/jsvi.1996.0776.
18. M. Alava and K. Niskanen. The physics of paper. *Reports on Progress in Physics*, 69(3):669–723, 2006.
19. U. Lee and H. Oh. Dynamics of an axially moving viscoelastic beam subject to axial tension. *International Journal of Solids and Structures*, 42(8):2381–2398, 2005.
20. T. Saksa, N. Banichuk, J. Jeronen, M. Kurki, and T. Tuovinen. Dynamic analysis for axially moving viscoelastic panels. *International Journal of Solids and Structures*, 49(23–24):3355–3366, 2012.
21. E. M. Mockensturm and J. Guo. Nonlinear vibration of parametrically excited, viscoelastic, axially moving strings. *ASME Journal of Applied Mechanics*, 72(3):374–380, 2005. DOI: 10.1115/1.1827248.
22. L.-Q. Chen and H. Ding. Steady-state transverse response in coupled planar vibration of axially moving viscoelastic beams. *ASME Journal of Vibrations and Acoustics*, 132:011009–1–9, 2010. http://dx.doi.org/10.1115/1.4000468.
23. L.-Q. Chen and B. Wang. Stability of axially accelerating viscoelastic beams: asymptotic perturbation analysis and differential quadrature validation. *European Journal of Mechanics – A/Solids*, 28(4):786–791, 2009. DOI: 10.1016/j.euromechsol.2008.12.002.
24. F. Gosselin, M. P. Païdoussis, and A. K. Misra. Stability of a deploying/extruding beam in dense fluid. *Journal of Sound and Vibration*, 299(1–2):123–142, 2007.
25. W. Lin and N. Qiao. The free vibration of rectangular plates. *International Journal of Solids and Structures*, 45(5):1445–1457, 2008.
26. I. A. Taleb and A. K. Misra. Dynamics of an axially moving beam submerged in a fluid. *AIAA Journal of Hydronautics*, 15(1):62–66, 1981.
27. A. D. Drozdov. Stability of a viscoelastic pipe filled with a moving fluid. *ZAMM – Journal of Applied Mathematics and Mechanics*, 77(9):689–700, 1997.
28. Z.-M. Wang, Z.-W. Zhang, and F.-Q. Zhao. Stability analysis of viscoelastic curved pipes conveying fluid. *Applied Mathematics and Mechanics*, 26(6):807–813, 2005.
29. T. Saksa, J. Jeronen, and T. Tuovinen. Stability of moving viscoelastic panels interacting with surrounding fluid. *Rakenteiden mekaniikka (Journal of Structural Mechanics)*, 45(3):88–103, 2012.
30. V. V. Bolotin. *Nonconservative Problems of the Theory of Elastic Stability*. Pergamon Press, New York, 1963.
31. Z. Sobotka. *Rheology of Materials and Engineering Structures*. Elsevier Science Ltd, Amsterdam, 1984.
32. F. Tisseur and K. Meerbergen. The quadratic eigenvalue problem. *SIAM Rev.*, 43:235–286, 2001.

Transcription of Discussion

ON TRAVELLING WEB STABILITY INCLUDING MATERIAL VISCOELASTICITY AND SURROUNDING AIR

Tytti Saksa,[1] *Juha Jeronen*,[1] *Nikolay Banichuk*[1,2] *and Matti Kurki*[3]

[1] Department of Mathematical Information Technology, P.O. Box 35 (Agora), FI-40014 University of Jyväskylä, Finland
[2] Institute for Problems in Mechanics, Russian Academy of Sciences, Prospekt Vernadskogo 101, 119526 Moscow, Russia
[3] JAMK University of Applied Sciences, P.O. Box 207, FI- 40101 Jyväskylä, Finland

Sören Östlund KTH

Could you, please, comment on the upstream boundary condition of a vanishing curvature? In elasticity, this would mean a vanishing bending moment.

Juha Jeronen

Actually, that is a good question. In the pure elastic case, of course, the second derivative corresponds to the bending moment, but this is not the case for a visco-elastic material, so we have just inserted this as a kinematic boundary condition. We have not considered what happens to the bending moment. There is a book by Wilhelm Flügge[5] which explains how to deal with the bending moment for a visco-elastic material. It is a bit more complicated than in the elastic case.

[5]Wilhelm Flügge, "Viscoelasticity", Springer-Verlag, Berlin-Heidelberg (1975), ISBN 978-3-662-02278-8, DOI 10.1007/978-3-662-02276-4.

Discussion

Bill Sampson University of Manchester (from the chair)

I'd like a clarification. You talked about the fact that your analysis was best suited for long and narrow draws and yet, of course, most draws in paper machines nowadays are short, and wide.

Juha Jeronen

Yes, that is true.

Bill Sampson

You have used a value of 0.6 metres for width, so, can you talk a bit about the applicability? You said that the shape should not be such a big deal, but then you chose a value for width typical of a narrow draw.

Juha Jeronen

Basically, if you want to analyse a short and wide draw, it is not possible to apply these techniques and you would need a more complicated model. So what we wanted to do here was to make a first step. This was fundamental academic research to see what happens. Since we had already earlier solved this fluid flow problem with a semi-analytical solution, we wanted to see what would happen if we introduced material visco-elasticity of the solid into the model, in the sense of building the model one step at a time.